JOURNAL OF SPACECRAFT AND ROCKETS
Vol. 43, No. 1, January–February 2006

Low-Thrust Trajectory Optimization Procedure for Gravity-Assist, Outer-Planet Missions

Byoungsam Woo* and Victoria L. Coverstone†
University of Illinois at Urbana–Champaign, Urbana, Illinois 61801
and
Michael Cupples‡
Science Applications International Corporation, Huntsville, Alabama 35806

A hybrid trajectory optimization procedure for a class of solar-electric-propulsion, gravity-assist, outer-planet missions is presented. The parameter space of a target mission is often nonconvex and a calculus-of-variations-based optimization algorithm suffers difficulties efficiently exploring this space. A hybrid procedure using a genetic algorithm to drive a calculus-of-variations program is developed to automate searching over a reduced parameter space. Employing the hybrid procedure, the delivered mass profiles of a Uranus and Pluto mission are generated more quickly than by using the calculus-of-variations optimization algorithm alone.

I. Introduction

WITH the success of the Deep Space 1 mission, solar-electric-propulsion (SEP) systems were ushered into the mainstream of propulsion system candidates for various interplanetary missions.[1,2] The long-duration, high-efficiency operation of SEP allows new ways to explore the inner and outer solar system and enables missions that can be difficult and expensive to reach with chemical propulsion systems. At the same time, SEP offers longer launch date opportunities than chemical counterparts.

In the exploration of outer-solar-system planets like Saturn or Neptune, intermediate planetary gravity assists have commonly been used because one or more gravity assists have the potential to save propellant.[3] Because of this advantage, many previous interplanetary missions (e.g., Voyager I, II; Galileo; Cassini; and NEAR) exploited the gravity assist.[4] This technique is used in this paper, employing a single Venus gravity assist to generate the trajectories to various outer planets. Venus has a short orbital period (225 days), and it is on average the closest planet to the Earth. These features provide at least yearly opportunities for a gravity assist, which increases launch-date flexibility in outer-planet missions. Earth shares similar advantages with Venus but is not considered in this paper. Although only one Venus gravity assist is investigated here, multiple Venus gravity assists as well as Earth gravity assists deserve an intensive analysis.

Generating a converged solution with SEP and a gravity assist using a calculus-of-variations (COV)-based optimization program can be a difficult and inefficient process. In addition, once a converged optimal solution is determined, there is no guarantee that the solution is the global optimum. Many trajectory optimization techniques have been developed and successfully applied to various continuous-thrust missions.[5,6] However, all methods have some difficulties in determining propellant-minimizing trajectories for SEP gravity-assist missions. The difficulty that accompanies a COV approach is the need for initial nonintuitive inputs to start the optimization, and there is no established method to provide the initial input that guarantees convergence. Among the current trajectory optimization programs, Solar Electric Propulsion Trajectory Optimization Program (SEPTOP)[7] is one of the most reliable programs and was validated on the SEP flight during the mission, Deep Space 1. SEPTOP is a COV-based low-thrust trajectory optimization program, and it determines a numerical solution to a two-point boundary-value problem that satisfies intermediate boundary constraints.[8] However, SEPTOP is not free from the usual difficulties of COV optimization programs and it depends heavily on user experiences in determining the initial input.

In addition, identifying a single local optimal trajectory is typically insufficient for a mission with a highly nonconvex parameter space. The local optimal trajectories from the different parts of the parameter space should be compared to highlight differences in mission characteristics. However, most COV-based optimization programs can only search the adjacent region of the given initial inputs, and so the resulting optimal trajectories have strong dependence on the initial inputs. Usually, searching the entire parameter space with brute force methods is far from efficient and practically impossible. In this paper, a genetic algorithm is employed in a hybridized manner with SEPTOP to improve the search efficiency with the capability to produce multiple locally minimizing solutions. At the same time, the parameter space is reduced by characterizing the optimal trajectories to concentrate the search effort to the desired region in the parameter space.

II. Hybrid Genetic-Algorithm/SEPTOP Procedure

Genetic algorithms have been used as search procedures for various optimization and machine-learning problems[9] and recently have also been employed in trajectory optimization investigations.[10,11] By combining a genetic algorithm and SEPTOP, it is possible to use the strong local optimizing ability of SEPTOP while exploring the large parameter space. A genetic algorithm is a robust search algorithm. However, if the parameter space is highly nonconvex, it will take extensive computations to thoroughly search, and it is quite possible to miss valuable solutions. In this paper, a method to reduce the parameter space is developed by characterizing existing optimal trajectories that were generated with SEPTOP alone. Then the hybrid procedure concentrates its searches to the smaller parameter space in order to better explore the region near the desired solution. Another advantage of this approach is a reduced searching time.

Figure 1 shows the procedure of hybrid optimization with the reduced parameter space. The characterization of optimal trajectories includes revolution-ratio (R-ratio) analysis, a constant SEP modeling, delivered mass estimation, phase calculation, and

Presented as Paper 2004-5397 at the AIAA/AAS Astrodynamics Specialist Conference, Providence, RI, 16–19 August 2004; received 18 November 2004; revision received 2 June 2005; accepted for publication 2 June 2005.

*Postdoctoral Researcher, Department of Aerospace Engineering, 104 S. Wright Street. Member AIAA.
†Professor, Department of Aeronautical and Astronautical Engineering, 104 S. Wright Street. Associate Fellow AIAA.
‡Lead Systems Engineer, In-Space Technology Assessment.

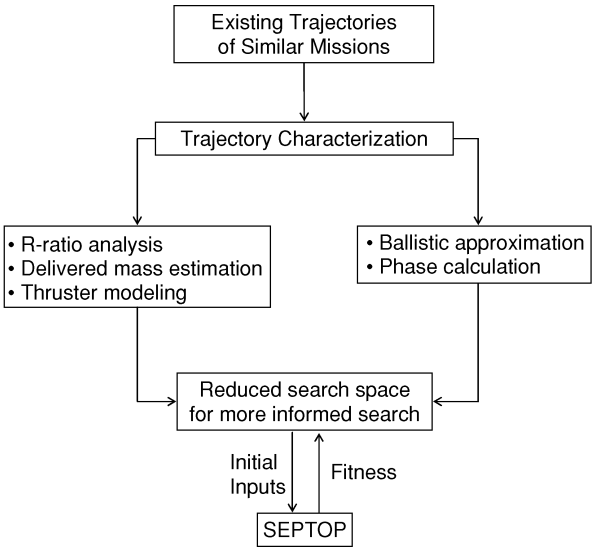

Fig. 1 Procedure of hybrid genetic-algorithm/SEPTOP trajectory optimization.

ballistic approximation of a portion of the SEP trajectory. A genetic algorithm searches the reduced space and generates initial inputs to drive SEPTOP, and SEPTOP returns the convergence error to the genetic algorithm as the measure of fitness of the initial input. The detailed description of the characterization appears in a later section.

In this paper, a simple genetic algorithm is used. The simple genetic algorithm uses three operators; selection, crossover, and mutation. To promote the diversity in the population, niching is also used. Niching penalizes solutions according to their degree of similarity to others in an attempt to distribute members over large portions of the parameter space and to avoid premature convergence to a single solution.

The hybrid, reduced parameter space procedure is applied to a class of SEP, outer-planet missions with a single Venus gravity assist. The arrival condition at the target planet is a flyby (matches position while velocity is unspecified). Aerocapture (or retrojet) is assumed in the missions,[12] but the mass of aerocapture equipment is not explicitly shown here. The hybrid genetic-algorithm/SEPTOP procedure can be applied to other types of missions that are difficult to obtain trajectories with SEPTOP alone. For example, the hybrid method was successfully used for a class of SEP, comet surface sample return mission to Tempel 1 with various thruster, power, and launch vehicles.[13] However, the reduction of the parameter space was not applicable for the Tempel 1 missions because there was no previous trajectory to characterize.

III. Characterization of Existing Trajectories

The target mission in this paper is a class of SEP, single Venus gravity-assist, outer-planet missions. These specified missions have been analyzed in the In-Space Propulsion Technology Investment Project as representative missions for comparing the effects of various system factors.[12] Table 1 shows the detail specifications of the target missions.[14,15] The characterization is performed from previously generated trajectories using SEPTOP for Saturn and Neptune missions. The resulting trajectory database serves to initiate the development of the hybrid procedure.

A. Revolution-Ratio

It is a common problem for any mission that utilizes a low-thrust (higher I_{sp}) onboard thruster and conventional launch vehicles (lower I_{sp}) to decide an optimal allocation of the launch and onboard propellants that minimizes the total propellant mass. The optimal propellant mass allocation between launch vehicle and onboard propulsion system is determined by the mission characterisitics, for example, the time of flight (TOF). For the target missions of this paper, the R-ratio conveniently represents the tradeoff between the launch and the SEP propellant. The definition of R-ratio is the number of revolutions of the gravity-assist planet for the number of revolutions of the spacecraft during the period from launch to gravity assist. For instance, a 3:1 R-ratio is one where roughly three gravity-assist planet years occur while the spacecraft makes roughly one revolution about the sun during the period from launch to gravity assist. Note that the integer number of R-ratio does not mean that the number of revolution is exactly an integer multiple of the planet year. A closest integer number is chosen to represent the revolutions of the gravity-assist planet and the spacecraft. If the spacecraft completes multiple heliocentric orbits prior to the gravity assist, larger integer numbers are used for the second figure of R-ratio (for example, 5:4 R-ratio). The R-ratio concept could be extended to the multiple gravity-assist missions, but it is not discussed in this paper.

Table 1 Specifications of target missions

Mission factor	Design value
Optimization	Maximize delivered mass to arrival planet
Departure planet	Earth
Arrival planet	Saturn, Uranus, Neptune, Pluto
Gravity assist	Single Venus gravity assist at 200-km altitude
Departure condition	Optimized C_3
Arrival condition	Flyby
Launch vehicle	Delta IV M + (4, 2)
SEP model[15]	4 thrusters + 1 spare 6.1 kWe at 3900 s I_{sp} 1.11-kWe minmum operation power
Power	25 kWe at 1 AU to SEP[a]

[a]AU = astronomical unit.

For the target missions, there exist optimal gravity-assist opportunities that differ almost exactly one Venus year (or multiple of one Venus year) from each other. These gravity-assist opportunities are locally optimal solutions even with the same TOF and launch epoch. Therefore, many optimal R-ratios (for example, 1:1, 2:1, 3:1, 4:1, and so on.) exist for an SEP, single Venus gravity-assist, outer-planet mission. Spiraling between the launch and gravity-assist planet is not considered in this paper because of the undesirable extended operational time of SEP. In a previous study,[14] the delivered mass in different R-ratio trajectories for a target mission can differ as much as 1000 kg. This difference is attributed to the different (but locally optimal) allocation of propellant mass between launch vehicle and onboard SEP system. Obtaining different R-ratio trajectories with SEPTOP alone is very time consuming because the different R-ratio solutions reside far from each other in the parameter space. The hybrid genetic-algorithm/SEPTOP procedure can obtain different R-ratio trajectories in a single batch run, and the search can be made more efficient by specifying the desired R-ratio and searching in a reduced parameter space.

B. Delivered Mass Estimation

The delivered mass estimation method for different R-ratio trajectories is developed to determine the targeted R-ratio for use in the hybrid technique. Also, this method aids in understanding the underlying fundamental differences between R-ratio trajectories. The method estimates the delivered mass of an R-ratio mission from an existing delivered mass profile of a different R-ratio mission based on a constant SEP thruster model and relations between propulsive energy and delivered mass. An SEP thruster has variable thrust profile while operating, but its performance can be closely approximated by a constant thrust profile for the target missions of this paper.[16] The constant SEP model has a constant I_{sp} of 3397 s (87% of the maximum I_{sp} of the I_{sp} 3900-s thruster) that is determined based on the previous trajectory data of similar missions with the thruster. Figure 2 shows the variation of delivered mass m_F in a Saturn and a Pluto missions for the variation of I_{sp} near the I_{sp} 3397 s. The delivered mass with variable SEP model is 2505 kg for the Saturn mission and 1213 kg for the Pluto mission. As shown in Fig. 2, the delivered mass can be closely approximated by the constant I_{sp} model, and, therefore, we can use the constant model in the delivered mass estimation method.

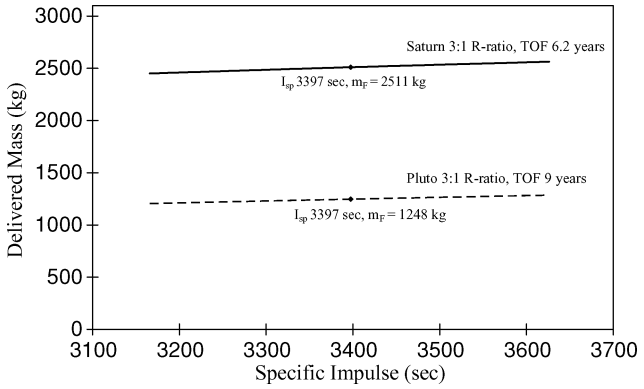

Fig. 2 Delivered mass sensitivity to the specific-impulse variation.

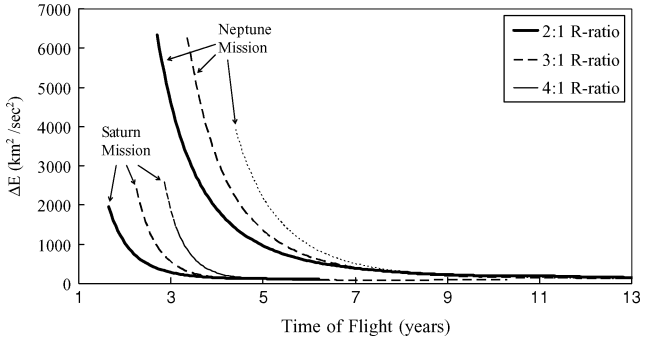

Fig. 3 Total propulsive energy increment vs time of flight.

The relation between the delivered mass and the total propulsive specific energy increment is constructed from existing trajectories of Saturn and Neptune missions.[14] For those missions, three different R-ratio trajectories were generated with SEPTOP. The total propulsive specific energy increment ΔE is defined as

$$\Delta E = \Delta V_{\text{SEP}}^2 + C_3 \tag{1}$$

where ΔV_{SEP} is velocity increment by SEP and C_3 is the square of the Earth-centered hyperbolic excess velocity of a spacecraft when it has just separated from the launch vehicle. The ΔV_{SEP} is computed by integrating the acceleration provided by the propulsion system along the trajectory. In Eq. (1), the ΔE excludes the energy increment provided by gravity assist caused by similarities in its value for the various missions that result from the gravity-assist planet and altitude being specified. Figure 3 shows the ΔE of three R-ratio trajectories for Saturn and Neptune missions. In Fig. 3, the ΔE curves for a target planet have similar shape regardless of the different R-ratio so the ΔE curves can be determined by a planar shift. The amount of the horizontal shifts (along with the TOF axis) is determined to be approximately one Venus year (224.7 days), and the amount of the vertical shifts (along with the ΔE axis) is found to be 30 km^2/s^2 between 3:1 and 2:1 R-ratios and 15 km^2/s^2 between 4:1 and 3:1 R-ratios. Figure 4 compares the 2:1 and 4:1 R-ratio ΔE curves from SEPTOP with the shifted 3:1 R-ratio ΔE curve for the Saturn mission. The close match of ΔE curves means that the ΔE curves in a target mission have similar profiles even with different R-ratios. This result is used in estimating the delivered mass of different R-ratio missions.

The delivered mass is computed from the shifted ΔE. Figure 5 shows the horizontal symmetry of the delivered mass and the ΔE for the 3:1 R-ratio, Saturn mission. With the horizontal symmetry, the delivered mass can be computed from ΔE with a scale factor and a constant. By representing the delivered mass $m_F(\xi)$ and $\Delta E(\xi)$ as functions of TOF ξ,

$$m_F(\xi) + k \cdot \Delta E(\xi) = C \tag{2}$$

where k is a scale factor between the delivered mass and ΔE, and C is the representing constant for the mission. Equation (2) is rearranged to be used in the linear least-square fit shown in Eq. (3):

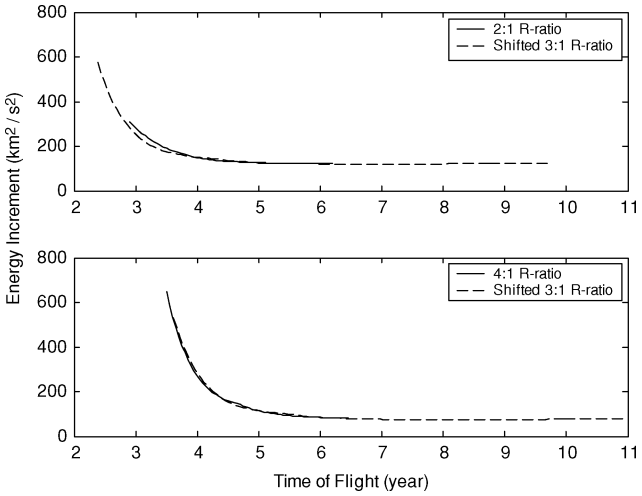

Fig. 4 Comparison of shifted ΔE in Saturn mission.

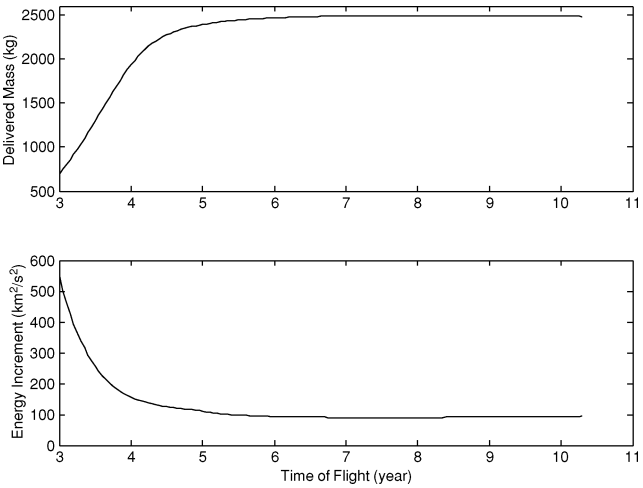

Fig. 5 Delivered mass and ΔE for 3:1 R-ratio, Saturn mission.

$$k \cdot \Delta E(\xi) - C = -m_F(\xi) \tag{3}$$

For the given TOF ξ_i, $i = 1, \ldots, n$, a linear least-square equation can be constructed.

$$\begin{bmatrix} \Delta E(\xi_1) & -1 \\ \vdots & \vdots \\ \Delta E(\xi_n) & -1 \end{bmatrix} \begin{pmatrix} k \\ C \end{pmatrix} = - \begin{pmatrix} m_F(\xi_1) \\ \vdots \\ m_F(\xi_n) \end{pmatrix} \tag{4}$$

The Q-R factorization[17] is used in solving Eq. (4) to calculate the k and C. From the existing data of Saturn and Neptune missions, the k and C are calculated and plotted with the inverse of semimajor axes of target planets in Figs. 6 and 7. In the figures, 2:1, 3:1, and 4:1 R-ratios are considered.

The k and C depend on the SEP and the launch vehicle because the relation between the ΔE and the delivered mass is determined from them. The k represents the propulsion efficiency in terms of the delivered mass. Large k means more efficient thrusting by the launch vehicle and SEP for the delivered mass. The constant C can be interpreted as the maximum delivered mass of the R-ratio trajectories to a target planet. With the interpretations of k and C, it is expected that the k and C are proportional to the inverse of the semimajor axis of a target planet. Therefore, the k and C of other target planets can be found by linear interpolation/extrapolation of existing data. In Figs. 6 and 7, the dotted lines are linear fitting of Saturn and Neptune mission data. In this paper, the k and C of

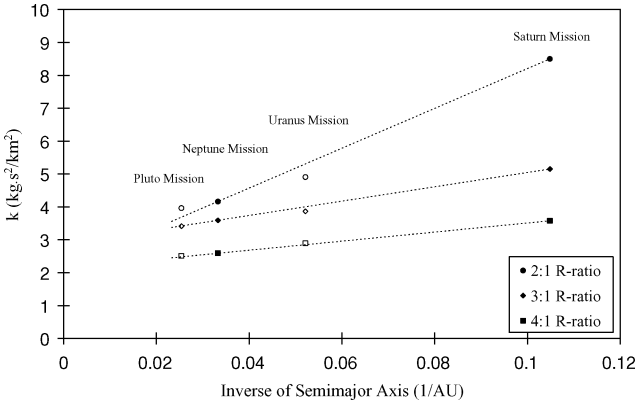

Fig. 6 The k as a function of inverse of semimajor axes.

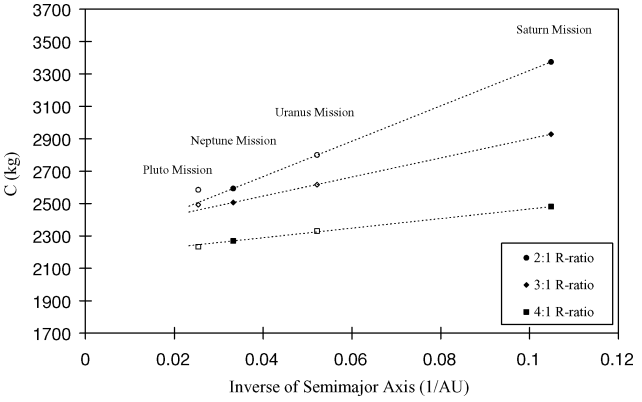

Fig. 7 C as a function of inverse of semimajor axes.

Uranus and Pluto missions are computed with their semimajor axes and the linear fitting lines. For comparison, the k and C computed from actual trajectory data are shown with hollow marks. It is clear that the linear interpolation generates close approximations for the k and C of Uranus and Pluto missions. The approximated k and C will be used in estimating the delivered mass of Uranus and Pluto missions. This k and C approximation is valid only for the target missions (SEP, single Venus gravity assist, and outer-planet flyby).

The delivered masses of Uranus and Pluto missions are estimated with the approximated k and C and planar-shifted ΔE curves. However, the procedure needs an initial ΔE curve of an R-ratio in each Uranus and Pluto mission to find the ΔE curves of the other R-ratio trajectories by a planar shifting. The initial ΔE curve can be generated by SEPTOP alone or by the hybrid genetic-algorithm/SEPTOP procedure.

Before estimating the delivered mass, note the incomplete horizontal symmetry in short TOF range in Fig. 5. This incomplete symmetry causes an error in the estimated delivered mass in the short TOF range so that the horizontal symmetry is not used for the short TOF range. Instead, the constant SEP model is used for the short TOF range. The estimation method with the constant SEP model uses a solution to the rocket equation[18] to compute the delivered mass m_F:

$$m_F = m_0 \exp(-\Delta V_{\text{SEP}}/c) \tag{5}$$

Here, the variable m_0 is the initial mass that is inserted into heliocentric orbit by a launch vehicle, and c is the exhaust velocity of SEP.

Figure 8 illustrates the process of the estimation method for the short TOF range. In the process, the ΔV_{SEP} and m_0 are approximated from the shifted ΔE profile, and the c is provided by the constant SEP model. The $C_3/\Delta E$ profile is used in approximating ΔV_{SEP} (or C_3) from the ΔE. In this paper, the $C_3/\Delta E$ profile is assumed to be similar in the short TOF range. The assumption is based on data from optimized Saturn and Neptune trajectories. Figure 9 shows the $C_3/\Delta E$ vs ΔE profile of Saturn and Neptune missions for the entire

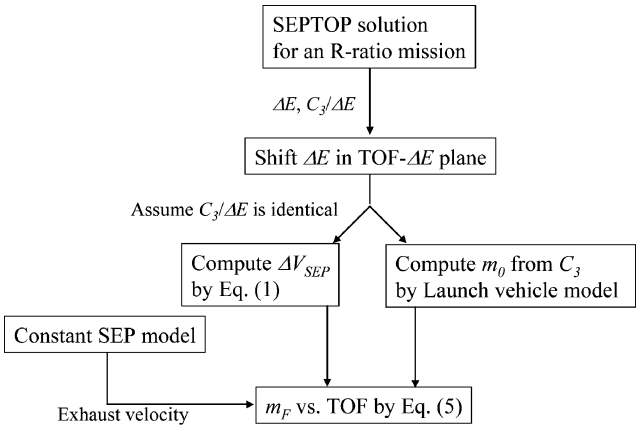

Fig. 8 Process of mass estimation method for short TOF range.

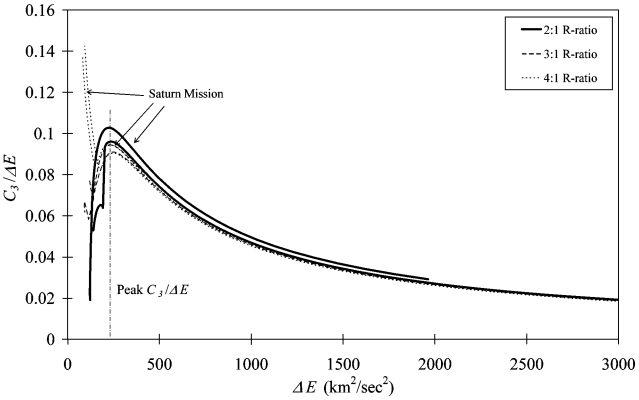

Fig. 9 $C_3/\Delta E$ vs ΔE for Saturn and Neptune mission, Magnified near peak.

TOF range. The $C_3/\Delta E$ profiles are very similar in short TOF range (right side of the peak $C_3/\Delta E$ in Fig. 9) but not in longer TOF range (left side of the peak $C_3/\Delta E$). Therefore, the estimation method with the approximated ΔV_{SEP} is used only for the short TOF range. In Fig. 9, the Saturn mission results are labeled, and the remaining unlabeled lines are the Neptune mission data.

The reason for the similar $C_3/\Delta E$ profile in different missions can be explained with the relative propulsive efficiency of the launch vehicle and the SEP. The percentage contributed by the launch and the SEP in ΔE is determined by their relative propulsion efficiency. All missions use the same launch vehicle and SEP system; therefore, similar $C_3/\Delta E$ profiles result for short flight-time missions. With the assumed $C_3/\Delta E$, C_3 becomes available from the shifted ΔE. Then we can compute ΔV_{SEP} by Eq. (1). The m_0 is also computed from the C_3 and a given launch vehicle model. Once we select a desired R-ratio based on the delivered mass estimation, the next step is to calculate the desired launch and gravity-assist time (phase of a trajectory) of the selected R-ratio trajectory for further reduction of the parameter space.

C. Phase Calculation Algorithm

The purpose of the phase calculation algorithm (PCA) is to select the launch and flyby dates as initial inputs for the hybrid genetic-algorithm/SEPTOP procedure. By selecting the dates, the parameter space is reduced significantly. The PCA is based on two characteristics of existing trajectories. The first characteristic is the geometrical regularity in the relative position of the Earth, Venus, and the target planets in the target mission trajectories. Figure 10 shows an optimal trajectory to Saturn with a 4:1 R-ratio and six years TOF. Three vectors are specified for a trajectory: the launch location, the Venus flyby location, and the arrival location. The transfer angle of each leg is defined as shown in Fig. 10.

To quantitatively establish the geometrical regularity, the locations of the launch, flyby, and arrival in the heliocentric coordinate

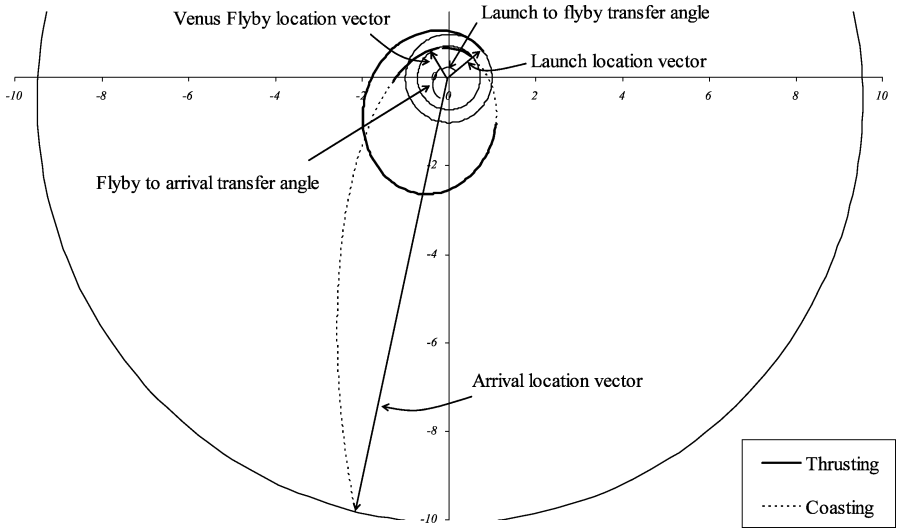

Fig. 10 Vectors of events locations, a 4:1 R-ratio Saturn trajectory.

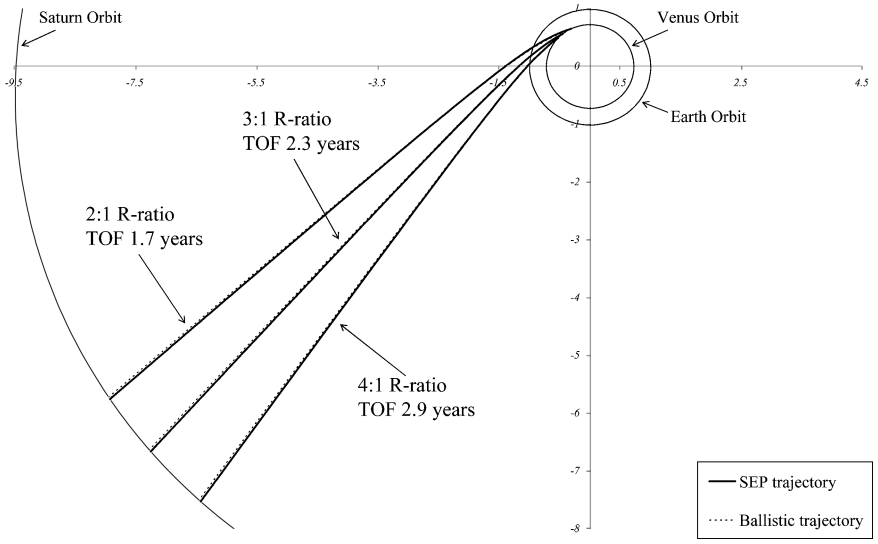

Fig. 11 Comparison between SEP and ballistic trajectories, Saturn mission.

frame are computed for the existing trajectories and consistency of the Venus flyby, and arrival locations in a target mission are seen to be strikingly similar even with a different R-ratio. This similarity holds true for different TOF missions when the TOF difference is not significant compared to the orbital period of the target planet. If the TOF difference is significant, the arrival location will be noticeably different. The second characteristic is the similarity between the SEP and ballistic trajectories for the gravity assist to the arrival planet leg. In the targeted missions, the SEP trajectory for the gravity assist to the arrival planet leg can be closely approximated by a ballistic trajectory because of the small thrusting arc in the early portion of this leg. The trajectory in Fig. 10 displays the large coasting arc prior to arriving at Saturn. In the target missions, an optimal trajectory tends to thrust near the sun because available power produces higher I_{sp}. Therefore, the SEP trajectory after the gravity assist is approximated with a ballistic trajectory in the PCA.

The first step in the PCA is to select a combination of the launch date (LD) and the Venus flyby date (FD) within a search span. The arrival date (AD) is determined easily by adding TOF to LD. The LD should be around the given nominal epoch (1 Jan. 2010 in this paper). Therefore, the search span for the LD is from 1 Jan. 2010 to 1 Jan. 2012 and is long enough to include the synodic period of the Earth and Venus (584 days). The FD search span is determined from the selected LD by Eq. (6):

$$\mathrm{LD} + (R_r - 1)Y_{\mathrm{Venus}} < \mathrm{FD} < \mathrm{LD} + 2(R_r - 1)Y_{\mathrm{Venus}} \qquad (6)$$

where R_r is the first number in the given R-ratio and Y_{Venus} is one Venus year. The FD range given in Eq. (6) is large enough to cover all target trajectories.

Once the LDs, FDs, and ADs are determined, the second step is to compute the ballistic trajectories for the FD to AD leg by solving a Lambert problem. To show the similarity between the SEP and ballistic trajectories, the trajectories are compared in Fig. 11 for Saturn missions with different R-ratios and TOFs. The ballistic approximation for the FD to AD leg also works successfully in other target missions.[16]

The final step is to compare the semimajor axes and flight-path angles of the ballistic trajectories with different combinations of the event dates. The semimajor axis is used in the comparison because it represents the orbital energy E of a trajectory as shown in Eq. (7):

$$\mathrm{E} = -\mu/2a \qquad (7)$$

where μ is the gravitational constant and a is the semimajor axis of the trajectory. In Eq. (7), a is a negative value because the approximating ballistic trajectories are hyperbolic for the target missions.[16] In this paper, the objective of the optimization is to maximize the delivered mass. The PCA searches the LD and FD combinations that have the larger $|a|$ of the ballistic trajectory. A large $|a|$ implies small orbital energy for the trajectory, which then in turn means a smaller required ΔV for the LD to FD leg. Figure 12 shows the semimajor

axes of ballistic trajectories for a Saturn mission with TOF 2.3 years and 3:1 R-ratio. With this R-ratio, the FD search span results in a range from two to four Venus years from a LD. The starting date for the LD scan is 1 Jan. 2010, whereas the search step of both the LD and the FD is five days. In Fig. 12, the semimajor axes are divided into three groups (A, B, and C). The B group has the smallest $|a|$, and so it is not considered as potential candidate solutions. Between the A and C groups, the C group is selected because the TOF from LD to FD is closer to three Venus years (with an average 2.3 Venus years) than the A group (with an average two Venus years). Note that group C is targeted to determine a R-ratio of 3:1 for this example.

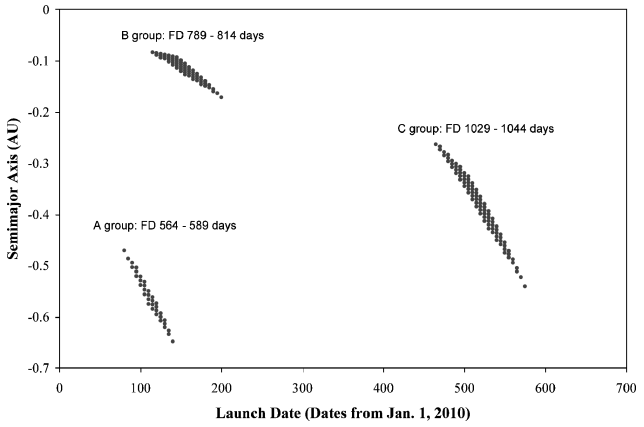

Fig. 12 Semimajor axes of ballistic trajectories for FD to AD leg, TOF 2.3 years, 3:1 R-ratio Saturn mission.

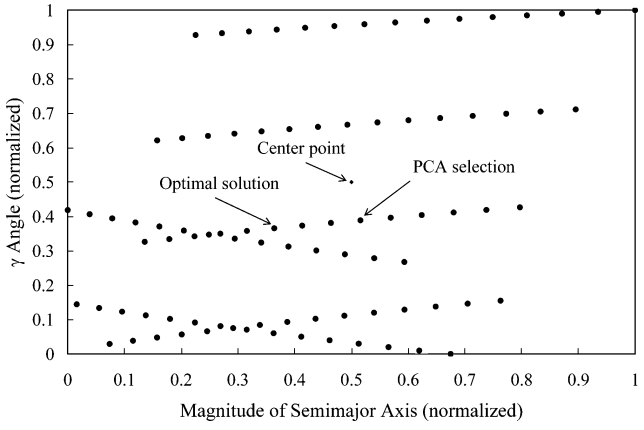

Fig. 13 Mapping of C group in $|a|$–γ plane, TOF 2.3 years, 3:1 R-ratio Saturn mission.

To select an initial input within the C group, we compare the flight-path angle γ of the outgoing asymptote. Figure 13 compares the members of the C group from Fig. 12 in the $|a|$–γ plane to select the member that is closest to the center of the plane because it primarily balances the different conditions about $|a|$ and γ. As will be shown, the center point member is a good initial input in most missions, but the PCA will be more accurate if the characteristics of each mission are considered. For example, a smaller R-ratio case tends to have larger $|a|$ because it has less time to accumulate the orbital energy before the flyby. Therefore, a point with a larger $|a|$ is better than the center point for a smaller R-ratio case. However, more research is required to include mission characteristics in the PCA. Currently, the PCA selects the closest member to the center point in the $|a|$–γ plane. For comparison, the optimal trajectory of the same mission is marked in Fig. 13.

To compare missions with different characteristics, the $|a|$ and γ values in Fig. 13 are normalized between 0 and 1 by subtracting the minimum values and then dividing the values with their range (maximum value–minimum value).

IV. Application of Hybrid Procedure with Characterization

A. Revolution-Ratio

In this paper, SEPTOP optimizes 13 parameters, and it needs initial inputs of these parameters to start the optimization. The parameters are LD, FD, C_3, B-plane angle, thrust switching function, and Lagrange multipliers about primer vectors at LD and FD. In a previous study, a set of different R-ratio trajectories is optimized with SEPTOP for Saturn and Neptune missions by optimizing the 13 parameters. Figure 14 illustrates typical trajectories from the previous study with the same TOF.[14] It shows that there exist multiple locally optimal trajectories with different R-ratio even with the same TOF.

B. Delivered Mass Estimation

The delivered mass estimation method is applied to Uranus and Pluto missions, 2:1 and 4:1 R-ratio trajectories. The k and C come from the linear fitting of Saturn and Neptune data. The ΔE and $C_3/\Delta E$ are generated from the existing 3:1 R-ratio trajectories of Uranus and Pluto missions. Figures 15 and 16 show the estimated delivered mass for Uranus and Pluto missions. For comparison, the actual delivered masses for the missions are also shown. The actual delivered mass data are generated later by the hybrid procedure to check the accuracy of the estimation method.

The estimated delivered mass consists of two parts, and their border is the peak $C_3/\Delta E$ point. In the figures, the estimation of delivered mass is accurate enough to decide which R-ratio is of interest. The maximum estimation error is less than 100 kg for the missions. The error comes from the assumptions about the horizontal symmetry, shifted ΔE profile, $C_3/\Delta E$ profile, and the SEP modeling error.

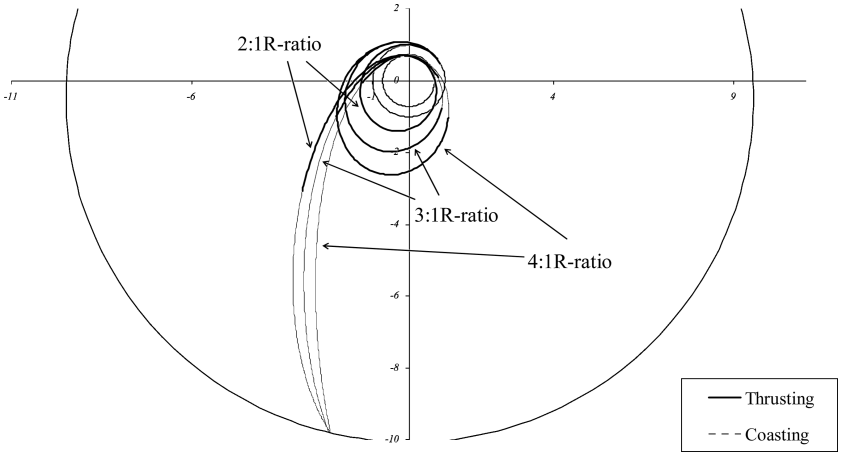

Fig. 14 Different R-ratio trajectories, TOF six years, Saturn mission.

Table 2 SEPTOP optimization results with LD, FD from PCA

Mission	R-ratio	TOF, year	Difference, LD, days	Difference, FD, days	Result
Saturn	2:1	1.7	30.4	10.4	Converged
	3:1	2.3	16.8	1.4	Converged
	4:1	2.9	26.2	5.5	Converged
Neptune	2:1	3.3	21.0	21.9	Converged
	3:1	3.8	5.0	0.7	Converged
	4:1	4.4	6.3	28	Converged to different solution
Uranus	2:1	2.7	2.7	1.9	Converged
	3:1	3.3	13.5	2.1	Converged
	4:1	3.9	19.2	4.7	Not converged
Pluto	2:1	3.4	9.3	5.4	Converged
	3:1	4.0	4.4	29.2	Converged
	4:1	4.6	16.8	11.4	Not converged

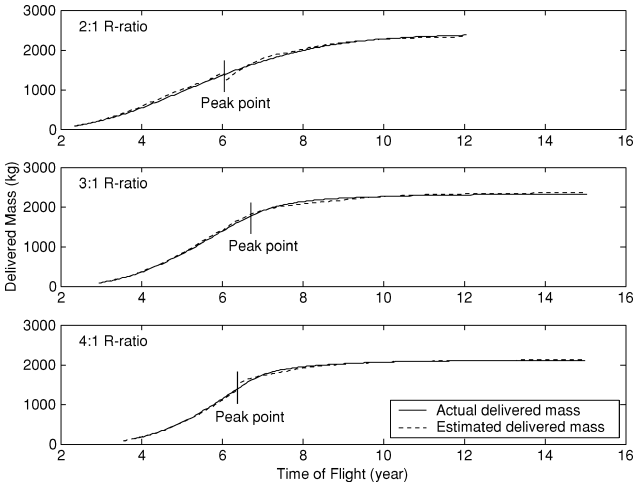

Fig. 15 Comparison of estimated and actual delivered masses, Uranus mission.

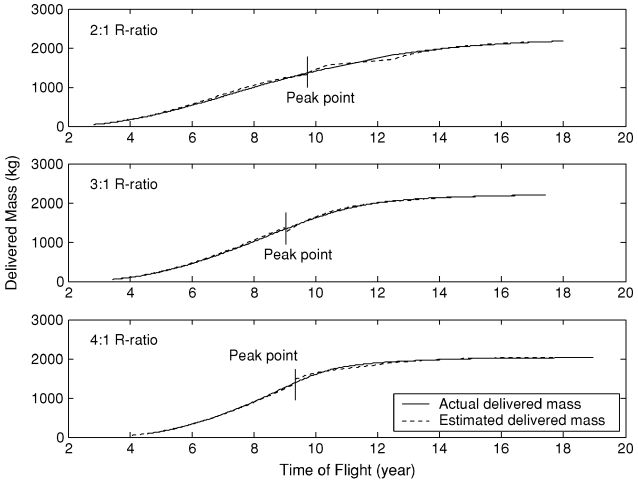

Fig. 16 Comparison of estimated and actual delivered masses, Pluto mission.

C. Phase Calculation Algorithm

Before applying PCA, the accuracy of the center point selection is investigated in several existing missions to Saturn and Neptune. The LD and FD from PCA replace the LD and FD of the existing SEPTOP solution. Then SEPTOP was ran to determine optimal trajectories with the replaced initial inputs to test whether it converges to the same solution. Table 2 summarizes the test results.

Table 2 also includes the test results for Uranus and Pluto trajectories. These trajectories were generated by the hybrid procedure, where the PCA approach was applied to validate the accuracy of the PCA selection in more missions. In Table 2, the PCA works successfully in nine out of the 12 test cases. The PCA selection converges to a slightly different trajectory in 4:1 R-ratio Neptune mission, but the trajectory is very similar to the original trajectory. The PCA selection does not converge in two cases because the trajectories reside in a very small area of convergence. Therefore, SEPTOP is unable to converge back to the original trajectories with the slightly different initial inputs of LD and FD. This result shows the difficulties of optimization in a highly nonconvex parameter space where multiple similar local optima can exist (as in 4:1 R-ratio Neptune mission of Table 2) and where the convex region around a solution can be very small (as in the two not converged cases).

Table 3 Control variables for hybrid procedure

Variable	Value
Number of parameters	11 or 13
Population size	150
Number of generations	50
Probability of crossover	1.0
Probability of mutation	0.0
Number of expected niches	25
Alpha	2.0

Table 4 Hybrid procedure test conditions and results, a Neptune mission

Parameter	First case	Second case
Genetic-algorithm search parameters	13	11
SEPTOP search parameters	13	11
Computation time, h	28.0	22.5
Number of converged individuals	40	27
Mission with different characteristics	2	5

D. Hybrid Genetic Algorithm/SEPTOP Procedure with Reduced Parameter Space

Table 3 shows the control variables of the hybrid procedure. The genetic algorithm has 150 individuals, and each individual has 13 parameters as the initial input of SEPTOP. The individuals who have the best combinations of these 13 parameters will produce converged solutions with SEPTOP, and they will survive and transfer their genes to the next generation.

The simple genetic algorithm searches for a better value for each parameter between the given lower and the upper bounds. If PCA provides LD and FD, then the hybrid procedure searches 11 parameters. The probabilities of crossover, mutation, and niching control variable alpha are selected based on experience.[11]

The hybrid procedure with reduced parameter space is applied to determine optimal trajectories for Uranus and Pluto missions. Figure 17 shows the resulting delivered masses of Uranus and Pluto missions. Figure 15 and 16 show the same data as a comparison of the estimated delivered mass. It took approximately one-eighth of the time to generate these results compared to the time took to generate the Saturn and Neptune data in a previous study.[14] A mission designer can choose the TOF and R-ratio of the actual trajectory based on the delivered mass profile.

To show the advantage of the reduced parameter space, a Neptune trajectory (TOF 3.8 year, 3:1 R-ratio case) was regenerated with the hybrid procedure. There are two test cases outlined in Table 4. In the first case, the hybrid procedure searches 13 parameters. In the second case, the PCA provides the LD and the FD so that an individual has 11 parameters. Then SEPTOP optimizes 11 parameters with the given LD and FD. By providing a good LD and FD to the hybrid procedure, we can concentrate the search efforts to the vicinity of the desired trajectory.

In Table 4, the computation time is measured on an Athlon 1.73-GHz personal computer. The converged individuals mean an individual that converges to an optimal solution with SEPTOP. These individuals are counted in the 50th generation. In the second case,

Table 5 Trajectory characteristics from the two hybrid procedures

Case	Mission	Delivered mass, kg	Propellant mass, kg	C_3, km^2/s^2	Launch date	Flyby date	R-ratio
1st	1	247.4	276.9	60.7	12/8/2010	3/5/2011	1:1
	2	175.5	421.3	58.6	9/6/2010	1/19/2011	1:1
2nd	1	175.2	473.8	57.1	10/1/2011	4/2/2012	1:1
	2	168.4	525.6	55.9	8/3/2010	7/14/2011	2:1
	3	247.4	276.9	60.7	12/8/2010	3/5/2011	1:1
	4	102.7	533.7	57.5	9/23/2010	6/9/2012	3:1
	5	157.1	548.0	55.6	9/12/010	9/3/2011	2:1

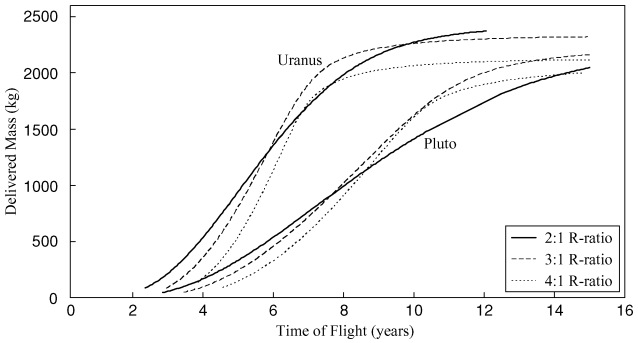

Fig. 17 Delivered mass of Uranus and Pluto missions.

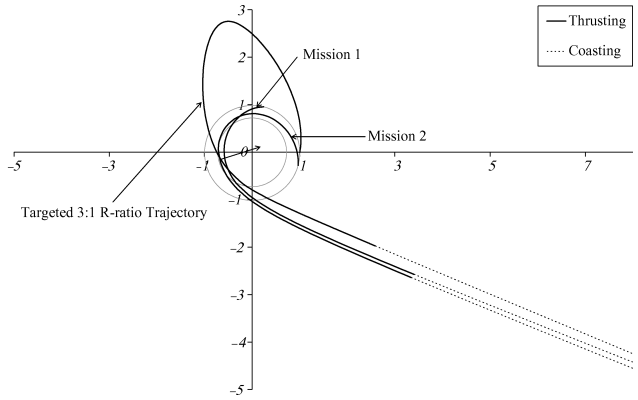

Fig. 18 Trajectories of the first test case, TOF 3.8 year, Neptune mission.

SEPTOP optimizes 13 parameters only at the last generation in order to find a trajectory with the optimized LD and FD. The number of missions with different characteristics represents the number of rationally different trajectories that SEPTOP generates with the converged individuals of the last generation. Table 5 summarizes the characteristics of the discovered optimal trajectories by the first and second test cases.

In Table 5, the mission 4 in the second case satisfies the R-ratio requirement. As a result, the mission 4 trajectory is identical to the trajectory that was targeted. Other missions have larger delivered mass than the mission 4, but they have a different R-ratio compared with the desired solution. Figures 18 and 19 show the trajectories of the first and second cases. Because of the relatively short TOF, there is no coast arc before the flyby in the trajectories.

Figure 18 also shows the trajectory that was targeted. The trajectories of missions 1 and 2 are smaller than the targeted trajectory because their R-ratios are smaller. In Fig. 19, the mission 4 trajectory is identical to the targeted trajectory. The trajectories of missions 2 and 5 are larger than the trajectories of missions 1 and 3 because their R-ratio is larger. As shown in Table 5, the hybrid procedure successfully discovers the target trajectory with the reduced parameter space. Table 5 also shows the existence of the multiple local optimal trajectories for a mission.

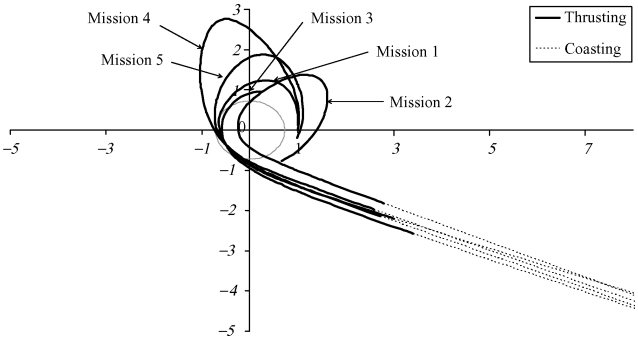

Fig. 19 Trajectories of the second test case, TOF 3.8 year, Neptune mission.

V. Conclusions

A hybrid procedure is developed and applied for a class of SEP, gravity-assist, outer-planet missions. The hybrid procedure utilizes a genetic-algorithm and a calculus-of-variations optimization program. The difficulties from the highly nonconvex parameter space of the target missions motivate the study of trajectory characterization for a more informed search. The optimal trajectories of previous research are characterized by their propulsion efficiency, R-ratio, and ballistic trajectory approximation. The delivered mass estimation method and the phase calculation algorithm are developed based on these characteristics. The delivered mass estimation method successfully generates the delivered mass of different R-ratio trajectories without performing an optimization. With the estimation results, the R-ratio trajectory to pursue in the hybrid procedure can be identified. The phase calculation algorithm generates good initial inputs for the launch and flyby date of an R-ratio trajectory. The generated launch and flyby dates are close to the optimal dates in many missions. The phase calculation algorithm provides the initial launch and flyby dates for the hybrid procedure. The hybrid procedure performs a more informed search with a desired R-ratio and good initial launch and flyby dates. Finally, the hybrid procedure was shown to generate a mission to Neptune with targeted characteristics.

Acknowledgments

The work described in this paper was supported by Science Applications International Corporation under contract with the NASA Marshall Space Flight Center (MSFC). Special thanks go to Les Johnson, Manager of NASA MSFC In-Space Propulsion Technology Investment Projects, and Randy Baggett, Manager of NASA MSFC Next Generation Electric Propulsion Technology Area, for providing encouragement and direction for this work.

References

[1]Rayman, M. D., and Williams, S. N., "Design of the First Interplanetary Solar Electric Propulsion Mission," *Journal of Spacecraft and Rockets*, Vol. 39, No. 4, 2002, pp. 589–595.

[2]Rayman, M. D., Chadbourne, P. A., Culwell, J. S., and Williams, S. N., "Mission Design for Deep Space 1: A Low-Thrust Technology Validation Mission," International Academy of Astronautics, Paper L98-0502, April 1998.

[3]Atkins, K. L., Sauer, C. G., and Flandro, G. A., "Solar Electric Propulsion Combined with Earth Gravity Assist: A New Potential for Planetary Exploration," AIAA Paper 76-807, Aug. 1976.

[4]Strange, N. J., and Longuski, J. M., "Graphical Method for Gravity-Assist Trajectory Design," *Journal of Spacecraft and Rockets*, Vol. 39, No. 1, 2002, pp. 9–16.

[5]Petropoulos, A. E., and Longuski, J. M., "A Shape-Based Algorithm for the Automated Design of Low-Thrust, Gravity-Assist Trajectories," American Astronautical Society, 01-467, July 30–Aug. 2001.

[6]Dickerson, W. D., and Smith, D. B., "Trajectory Optimization for Solar-Electric Powered Vehicles," *Journal of Spacecraft and Rockets*, Vol. 5, No. 8, 1968, pp. 889–895.

[7]Sauer, C. G., Jr., "Optimization of Multiple Target Electric Propulsion Trajectories," AIAA Paper 73-205, Jan. 1973.

[8]Williams, S. N., "An Introduction to the Use of VARITOP A General Purpose Low-Thrust Trajectory Optimization Program," Jet Propulsion Lab., D-11475, Pasadena, CA, 1994.

[9]Goldberg, D. E., "Genetic and Evolutionary Algorithms, Come of Age," *Communications of the ACM*, Vol. 37, No. 3, 1994, pp. 113–119.

[10]Rauwolf, G., and Coverstone, V. L., "Near-Optimal Low-Thrust Orbit Transfers Generated by a Genetic Algorithm," *Journal of Spacecraft and Rockets*, Vol. 33, No. 6, 1996, pp. 859–862.

[11]Hartmann, J. W., Coverstone, V. L., and Williams, S. N., "Optimal Interplanetary Spacecraft Trajectories via a Pareto Genetic Algorithm," *Journal of the Astronautical Science*, Vol. 46, No. 3, 1998, pp. 267–282.

[12]Cupples, M., Green, S., and Coverstone, V. L., "Factors Influencing Solar Electric Propulsion Vehicle Payload Delivery for Outer Planet Missions," American Astronautical Society, Paper 03-123, Feb. 2003.

[13]Cupples, M., Coverstone, V. L., and Woo, B., "Application of Solar Electric Propulsion to a Comet Surface Sample Return Mission," AIAA Paper 2004-3804, July 2004.

[14]Woo, B., Coverstone, V. L., Hartmann, J. W., and Cupples, M., "Trajectory and System Analysis for Outer-Planet Solar Electric Propulsion Missions," *Journal of Spacecraft and Rockets*, Vol. 42, No. 3, 2005, pp. 510–516.

[15]Patterson, M., Foster, W. T., Rawlin, J. E., Roman, V., Robert, F., and Soulas, G., "Development Status of a 5/10-kW Class Ion Engine," AIAA Paper 2001-3489, July 2001.

[16]Woo, B., "Efficient Trajectory Optimization Procedure for Designing Solar-Electric Propulsion, Gravity-Assist Outer-Planet Missions," Ph.D., Dissertation, Dept. of Aerospace Engineering, Univ. of Illinois, Urbana. IL, Sept. 2004.

[17]Heath, M. T., *Scientific Computing An Introductory Survey*, 2nd ed., McGraw–Hill, Boston, 2002, pp. 120–131.

[18]Prussing, J. E., and Conway, B. A., *Orbital Mechanics*, Oxford Univ. Press, New York, 2001, Chap. 12.

C. Kluever
Associate Editor